

AD-A045 997

EMMANUEL COLL BOSTON MASS

F/G 14/2

CALIBRATION OF THE SSJ/3 SENSOR ON THE DMSP SATELLITES.(U)

SEP 77 A HUBER, J PANTAZIS, A L BESSE

F19628-76-C-0039

UNCLASSIFIED

SCIENTIFIC-2

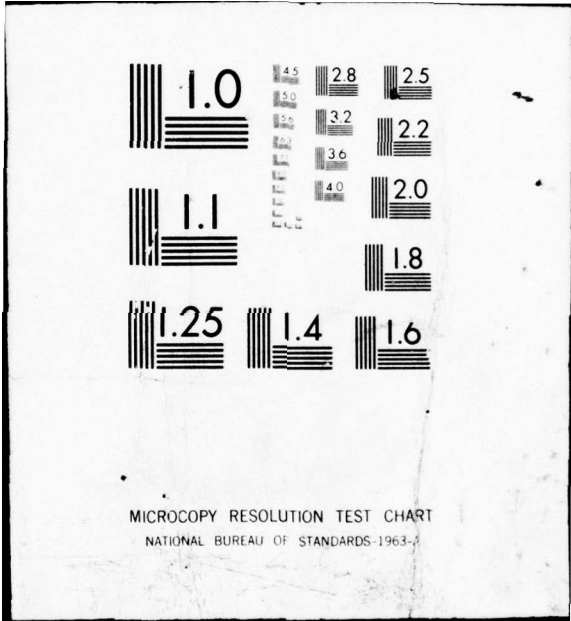
AFGL-TR-77-0202

NL

| OF |
AD
A045997



END
DATE
FILMED
11-77
DDC



AD A 045997

12

AFGL-TR-77-0202 ✓

CALIBRATION OF THE SSJ/3 SENSOR ON THE DMSP SATELLITES

ALAN HUBER
JOHN PANTAZIS
A.L. BESSE
P.L. ROTHWELL

THE TRUSTEES OF EMMANUEL COLLEGE ✓
400 THE FENWAY
BOSTON MASSACHUSETTS 02115

SEPTEMBER 1977

SCIENTIFIC REPORT NO. 2 ✓

APPROVED FOR PUBLIC RELEASE; DISTRIBUTION UNLIMITED

AD No. _____
DDC FILE COPY

AIR FORCE GEOPHYSICS LABORATORY
AIR FORCE SYSTEMS COMMAND
UNITED STATES AIR FORCE
HANSCOM AFB, MASSACHUSETTS 01731

DDC
RECEIVED
NOV 4 1977
B

Qualified requestors may obtain additional copies from the Defense Documentation Center. All others should apply to the National Technical Information Service.

UNCLASSIFIED

SECURITY CLASSIFICATION OF THIS PAGE (When Data Entered)

19 REPORT DOCUMENTATION PAGE		READ INSTRUCTIONS BEFORE COMPLETING FORM	
18 19 REPORT NUMBER AFGL TR-77-0202	2. GOVT ACCESSION NO.	3. RECIPIENT'S CATALOG NUMBER	
6 4. TITLE (and Subtitle) CALIBRATION OF THE SSJ/3 SENSOR ON THE DMSP SATELLITES.	14 5. TYPE OF REPORT & PERIOD COVERED SCIENTIFIC 18-2 01APR77 - 01SEP77	6. PERFORMING ORG. REPORT NUMBER	
10 7. AUTHOR ALAN/HUBER, A.L./BESSE JOHN/PANTAZIS, P.L./ROTHWELL	15 8. CONTRACT OR GRANT NUMBER(s) F19628-76-C-0039		
9 9. PERFORMING ORGANIZATION NAME AND ADDRESS EMMANUEL COLLEGE 400 THE FENWAY BOSTON MA 02115	16 10. PROGRAM ELEMENT, PROJECT, TASK AREA & WORK UNIT NUMBER 61102F 2311G102	17 11 12. REPORT DATE SEPTEMBER 1977	17 13. NUMBER OF PAGES 42
11 11. CONTROLLING OFFICE NAME AND ADDRESS AIR FORCE GEOPHYSICS LABORATORY HANSCOM AFB MA 01731 CONTRACT MONITOR: ROBERT C. FILZ (PHG)	14 14. MONITORING AGENCY NAME & ADDRESS (if different from Controlling Office) Rept. for 1 Apr - 1 Sep 77	15 15. SECURITY CLASS. (of this report) UNCLASSIFIED	15a 15a. DECLASSIFICATION DOWNGRADING SCHEDULE
16. DISTRIBUTION STATEMENT (for this Report) A - APPROVED FOR PUBLIC RELEASE; DISTRIBUTION UNLIMITED 12 43p.			
17. DISTRIBUTION STATEMENT (of the abstract entered in Block 20, if different from Report) DDC RECEIVED NOV 4 1977 B			
18. SUPPLEMENTARY NOTES *PHYSICS RESEARCH DIVISION, EMMANUEL COLLEGE			
19. KEY WORDS (Continue on reverse side if necessary; and identify by block number) SSJ/3 SENSOR MONTE CARLO CODE CHANNELTRON ELECTROSTATIC ANALYZER			
20. ABSTRACT (Continue on reverse side if necessary and identify by block number) The SSJ/3 sensor is designed to measure electrons from 50 eV to 20 keV. This is accomplished by using two head assemblies with common signal processing and voltage sources. The low-energy head assembly selects 50.0 to 1,000 eV electrons over eight channels with a normalization factor $H = 4.3 \times 10^{-5} \text{ cm}^2$ ster. The high-energy assembly similarly selects 1.00 to			

DD FORM 1 JAN 73 1473 EDITION OF 1 NOV 65 IS OBSOLETE

UNCLASSIFIED

SECURITY CLASSIFICATION OF THIS PAGE (When Data Entered)

128 950

LB

0.000043 50 CM

MIL-STD-847A
31 January 1973

UNCLASSIFIED

SECURITY CLASSIFICATION OF THIS PAGE(When Data Entered)

20.0 keV electrons over eight channels with an H-factor equal to 1.30×10^{-5} cm²-ster.

Energy resolution is approximately 10% for an isotropic incident flux. An electron beam was used to determine angular and energy response. These measurements were compared with results from a Monte-Carlo computer code and approximate analytic methods to determine the final normalizations.

ADDITIONAL INFORMATION

NTIS	WIDE DISTRIBUTION	✓
DDC	DDC SECTION	✓
UNCLASSIFIED		✓
AVAILABILITY		

BY

DISTRIBUTION/AVAILABILITY

Dist. AVAIL. AND/OR OFFICIAL

A		
---	--	--

UNCLASSIFIED

SECURITY CLASSIFICATION OF THIS PAGE(When Data Entered)

TABLE OF CONTENTS

	<u>PAGE</u>
Figure Captions (Page No.)	4
I Introduction	5
II Instrument Design	6
III Techniques Used in Calibration	8
IV Results	10
Table 1	14
Table 2	15
Acknowledgements	16
Figures 1-11	17-27
Appendix A	28
Appendix B	30
Appendix C	31
Computer Program Used for Monte Carlo Computations	
References	42

FIGURE CAPTIONS

- Figure 1. The SSJ/3 instrument and associated electronic boards. The rectangular slits are entrance apertures for electrons. Behind the small circular hole is a UV detector that causes the channeltron acceleration voltage to be turned off when viewing the sun.
(17)
- Figure 2. Detailed photograph of the SSJ/3 head assembly board. a $\frac{1}{2}$ " block is also shown for comparison. The narrowly separated plates select the high-energy electrons. The widely separated plates select the lower energy electrons.
(18)
- Figure 3. Detailed schematic sketch of a detector assembly. Also given are the relevant dimensions for each set of plates.
(19)
- Figure 4. Schematic of the electronic logic used in SSJ/3.
(20)
- Figure 5. Comparison between measured and Monte-Carlo results for a normally incident beam. Energies are off-set for ease of display.
(21)
- Figure 6. Angular response of the high-energy plates in the R-plane (α).
(22)
- Figure 7. Angular response of the low energy plates in the R-plane (α).
(23)
- Figure 8. Angular response of the high-energy plates in the plane parallel to the plates (β).
(24)
- Figure 9. Angular response of the low energy plates in the plane parallel to the plates (β).
(25)
- Figure 10. Theoretical response of the high-energy plates to an isotropic incident flux. Use Table 2 for channel 8 mid-point energy. Final normalization is also shown.
(26)
- Figure 11. Theoretical response of the low energy plates to an isotropic incident flux. Use Table 2 for channel 9 mid-point energy. Final normalization is also shown.
(27)

I. INTRODUCTION

The calibration of the SSJ/3 sensor was carried out using both experimental and theoretical techniques. Experimental measurements were compared with predictions from a Monte Carlo particle tracing code and from analytic approximations.

In Section II instrument design is discussed. Section III described techniques used in calibration while Section IV describes the logic used to obtain the final normalization values.

II. INSTRUMENT DESIGN

Introduction. The SSJ/3 instrument package is shown in Figures 1 and 2. Figure 1 shows the instrument case and the associated electronic boards. The apertures on the case are directly in front of the particle collimators that are shown in the bottom of Figure 2. Behind the collimators are curved cylindrical plates. The plate separation and the applied voltage determine the energy band of the transmitted electrons. The electrons, after passing through the exit collimator, are detected by the C-shaped Channeltron Electron Multiplier detectors that are also shown in Figure 2.

Head Assembly. Electrostatic analyzers (ESA's) select charged particles by applying a voltage between two concentric plates. The SSJ/3 instrument uses two sets of cylindrical concentric plates as shown in Figure 2. Charged particles of the proper sign and energy have trajectories that are almost parallel to the plate surfaces. Particles of greater or lesser energy impinge on the plate surfaces. The mean energy E can be easily derived by requiring a balance between electrostatic and centrifugal accelerations. For plates of radii r_1 and r_2 ($r_2 > r_1$) and an applied voltage difference of V , E is given by

$$E = \frac{eV}{2 \ln(r_2/r_1)} \quad (1)$$

If V is fixed then the detected energy is determined by the ratio of r_2 to r_1 . This explains the larger plate separation, ΔR , for the lower energy detector assembly as tabulated in Figure 3. The sector angle of the plates and their separations, together with aperture and exit slits, determine the

transmission efficiency. Additional baffles are placed in the aperture assembly to eliminate sunlight (UV) scatter into the detectors.

Behind the exit aperture, the two channeltrons are mounted as shown in the lower righthand corner of Figure 2. Electrons impinging on the cone-shaped area produce secondaries which cascade through the channeltron producing a detectable pulse at the end. This pulse is then processed by the instrument's internal electronics. Channeltron operating lifetime is extended by shutting off the accelerating potential whenever the instrument is looking at the sun. This is done by a small phototransistor mounted adjacent to the instrument apertures. See Figure 1. In Figure 3 is a schematic representation of the SSJ/3 head assemblies and gives the relevant dimensional values.

Electronic Logic. Figure 4 shows the electronic logic. The channeltron outputs (DET L and DET H) are amplified and then counted in nine-bit logarithmic counters. A complete 16-channel energy spectrum is read out every second. Appendix A describes in detail the conversion of the logarithmic counter to decimal form. The same programmable power supply is used for biasing both sets of plates. The voltage difference for each set of plates is obtained by applying $\pm V/2$ to each plate.

III. TECHNIQUES USED IN CALIBRATION

Experimental. Experimental calibrations were made using accelerated electrons from a Tritium source. After acceleration by an applied voltage, the beam was collimated so that a mono-energetic, unidirectional source was incident on the instrument apertures. A turntable enclosed in a vacuum system provided mobility for angular response measurements. The beam was found to have an energy dispersion which was negligible in comparison with the instrument's response. By changing the applied voltage various energies could be selected.

Theoretical Approximations. Geometric considerations lead to the following results: 1) If a and b are the heights of the entrance and exit apertures of the collimator and ℓ is the separation then between them such that $\ell \gg a + b$, then the angular resolution, $\Delta\beta$, is to a good approximation given by $\Delta\beta \approx (a + b)/\ell$. This approximation works well for the direction parallel to the plates, but not for the orthogonal component. 2) The geometric factor ($\text{cm}^2\text{-sec}$) for a long rectangular collimator is approximated by

$$G = \frac{A_1 \times A_2}{\ell^2}$$

A_1 = area of collimator entrance aperture

A_2 = area of collimator exit aperture

ℓ = distance between apertures

This formula provides a rapid means of obtaining a "ballpark" estimate for the geometric factor of a rectangular collimator. We used, however, the exact expression given in Appendix B in deriving our final results.

Monte Carlo Program. In Appendix C is a listing of the Monte Carlo computer code used to analyze instrument response. The basic idea is to trace electrons through the instrument to determine if they hit the channeltron. In this manner the

effect of design can immediately be recognized.

Input data includes aperture geometry, plate radii, arc length of plates, plate voltage, channeltron size, and the position of the aperture and channeltrons relative to the plates. A retarding potential can also be inputted which impedes secondary electrons produced in the plates from hitting the channeltrons. Provision has also been made to examine elastic scattering off the plate surfaces. This feature will not be used.

Let us now consider an isotropic flux, J , incident on the outside aperture. The number of incident particles per unit area is given by

$$dN = J \sin\theta \cos\theta d\theta \quad (1)$$

or if R is a random number over the interval 0-1 then the relation

$$\theta = \frac{1}{2}\cos^{-1}(1-2R) \quad (2)$$

generates the appropriate angular distribution of incident particles.

As a test we generated 6×10^5 particles through the high-energy collimator using equation (2). The theoretically calculated geometric factor for this collimator (1.8 cm high x 0.2 cm wide x 1.15 cm long) is $0.0622 \text{ cm}^2/\text{sr}$ (Appendix B). The "measured" geometrical factor using particle tracing was found to be $0.0624 \text{ cm}^2/\text{sr}$ which agrees with the theoretical value to within 0.32%. This result confirms that the computer code was properly simulating an incident isotropic flux through the collimator.

IV. RESULTS

The Method. Instrument calibration is determined by comparing the predicted (Monte Carlo) response curves with the measured ones. First, we look at the energy resolution for a normally incident beam. Then angular response is examined in directions parallel and perpendicular to the plates. After showing substantial agreement with experimental data, the Monte Carlo code is used to calculate the final normalizations for an incident, isotropic flux. Comparisons are made with results from approximate analytic techniques. Channeltron detection efficiency as a function of incident electron energy is also discussed and included.

Throughout this section we use energy channels 8 and 9 to determine the response properties of the two head assemblies.

Energy Resolution. In Figure 5 the Monte-Carlo and experimental results are shown for a normally incident electron beam. The beam energy was systematically scanned across the channel to obtain the energy response curve. It is seen from Figure 5 that the Monte Carlo and experimental results are in excellent agreement.

Angular Response. Figure 6 shows the angular response (α) of the high energy plates in the plane perpendicular to the plates (R-plane). In this case the measured resolution is somewhat wider than that predicted by Monte Carlo. This effect is probably due to scattering off the plate surface. Figure 7 shows a similar response curve for the low-energy plates. Observe that there are fewer measured particles than predicted at large positive angles. This effect is probably from fringe electric field resulting from larger plate separation. See Figure 2. The triangular shape of the theoretical response curve indicates that the front collimator

is the dominant determinant of the angular response.

Now we look at the angular response (β) in the plane parallel to the plate surfaces. All angular response curves are determined at the central (peak) channel energy. Figure 8 shows the appropriate curves for the high energy (narrowly separated) plates. Note that while the resolution is in excellent agreement, there is a systematic shift of about 2.5° . Because the resolution is about 8.0° , we do not consider this error as being serious. Figure 9 shows similar curves for the low energy (widely separated) plates. Here there is also a systematic shift of about 1.25° . Note that for both angular scans the measured resolutions for the low energy plates are less than the predicted ones. This is opposite to what one would normally expect and indicates a slight systematic error.

Final Normalizations. The final normalizations were determined using the Monte Carlo program. As described previously, an isotropic flux is taken incident on the front aperture. One thousand electrons are traced through the plates at each energy. Figure 10 and 11 show the results for channels 8 and 9 respectively. The ordinate represents the percentage of electrons that are detected after leaving the collimator (i.e. the transmission efficiency through the plates). The integral of this curve times the aperture G-factor gives the final normalizations.

For an incident flux J the count rate (CR) is given by

$$JG = CR$$

where G is the normalization factor in $\text{cm}^2/\text{sr}/\text{ev}$. The G-factor can be approximated by

$$G \approx A \Omega \Delta E$$

A = area of entrance aperture

Ω = acceptance solid-angle

E = energy bandwidth

Dividing by the center energy E we have

$$H = G/E \approx A \Omega \frac{\Delta E}{E}$$

Now since A, Ω and $\Delta E/E$ are constant for each set of plates, then this one number H characterizes the normalization for all channels. For the high-energy (narrowly separated plates) channels $H = 1.30 \times 10^{-4} \text{ cm}^2/\text{sr}$. For the low-energy (widely-separated plates) $H = 4.3 \times 10^{-5} \text{ cm}^2/\text{sr}$.

We now compare this result with an approximate analytic approach. In this approach it is assumed that the energy and angular response curves are independent gaussian distributions. The final normalization is the integral product of these distributions. The result is

$$H = 1.20 A \epsilon R_0 \Delta\alpha\Delta\beta$$

where A is the aperture area, R_0 is the channeltron detection efficiency (at $E \sim 1 \text{ keV}$, $\epsilon = 1$), R_0 is $\Delta E/E$, $\Delta\alpha$ and $\Delta\beta$ are the FWHM (full-width half maximum) of the angular response curves.

Using the measured results tabulated in Table 1, this approximation gives us $H = 6.8 \times 10^{-5} \text{ cm}^2/\text{sr}$ for the high energy plates and $H = 5.55 \times 10^{-5} \text{ cm}^2/\text{sr}$ for the low energy plates. Note, however, that energy and angular resolutions are not independent for this particular electrostatic analyzer, contrary to the assumptions in the approximate approach.

A wide collimator allows more electrons at various energies to reach the channeltrons. A narrow collimator allows fewer electrons to reach the detectors over a narrower energy bandwidth. This effect is seen by comparing Figure 5 with Figures 10 and 11. The energy resolution of the high-energy plates is 2.3 times greater for an isotropic flux than for a normally incident flux. For the low energy plates it is 1.5 times greater. We interpret this difference to be due to the collimator in front of the high energy plates having a G-factor 16 times that of the one in front of the low-energy plates. It is for this reason we consider the Monte Carlo normalization as more closely reflecting realistic fluxes.

The final normalization values for each energy channel as given in Table 2. Dividing the count rate by the approximate normalization gives the equivalent flux in electrons per $\text{cm}^2/\text{sr}/\text{ev}/\text{sec}$. The channeltron efficiencies were obtained from Archuleter and DeForest (1971). For $1 \text{ keV} \leq E \leq 50 \text{ MeV}$, $\epsilon = 1.0 - 2.0/(3.0 + 6.5/(E - 0.5) + 30.0/(E - 0.5)^3)$ where E is expressed in keV. For $10 \text{ ev} \leq E \leq 70 \text{ eV}$ ϵ was taken to be

$$\epsilon = 0.10 E^{0.515} \text{ (E in ev)}$$

Note that the midpoint energies in Figures 10 and 11 are not the same as in Table 2, which are the final calibrated values. This does not affect H, however, which is energy-independent. The stated errors in Table 2 for the various energy channels are a best estimate from electronic and experimental uncertainties.

TABLE 1

Measured Energy and Angular Resolutions With a
Monoenergetic and Unidirectional Electron Beam

	<u>Channels 1-8</u>	<u>Channels 9-16</u>
$\Delta\alpha$	$1.6\pm 0.2^\circ$	$3.7\pm 0.7^\circ$
$\Delta\beta$	$8.0\pm 0.8^\circ$	$4.75\pm 0.08^\circ$
$\Delta E/E(R_o)$	$4.0\pm 0.4\%$	$7.2\pm 0.4\%$
G (Aperture)	$6.22\times 10^{-2}\text{cm}^2\text{-sr}$	$3.929\times 10^{-3}\text{cm}^2\text{-sr}$

TABLE 2

SSJ/3 Normalizations

$$H = 1.30 \times 10^{-4} \text{ cm}^2\text{-sr}$$

<u>Channel Number</u>	<u>Center Energy (eV)</u>	<u>Channeltron Efficiency ϵ</u>	<u>G = HEϵ Normalization (G) HEϵ(cm²-sr-eV)</u>
1	20,000±3%	0.405	1.05x10 ⁰
2	13,700±3%	0.43	7.66x10 ⁻¹
3	8,990±3%	0.48	5.59x10 ⁻¹
4	5,500±3%	0.56	4.00x10 ⁻¹
5	3,790±3%	0.66	3.25x10 ⁻¹
6	2,290±3%	0.83	2.47x10 ⁻¹
7	1,590±5%	0.94	1.94x10 ⁻¹
8	1,060±6%	0.99	1.36x10 ⁻¹

$$H = 4.3 \times 10^{-5} \text{ cm}^2\text{-sr}$$

9	1,045±3%	1.00	4.49x10 ⁻²
10	661±3%	1.00	2.84x10 ⁻²
11	434±3%	1.00	1.86x10 ⁻²
12	264±3%	1.00	1.13x10 ⁻²
13	183±3%	1.00	7.86x10 ⁻³
14	110±3%	1.00	4.73x10 ⁻³
15	77±5%	1.00	3.31x10 ⁻³
16	51±6%	.76	1.67x10 ⁻³

ACKNOWLEDGEMENTS

We would like to express our appreciation to Dr. Davis Nelson of Aerospace Corporation who substantially contributed to many of the design features. In addition we would like to express our gratitude to the Space Physics Laboratory at Aerospace Corporation for the use of their calibration facilities.

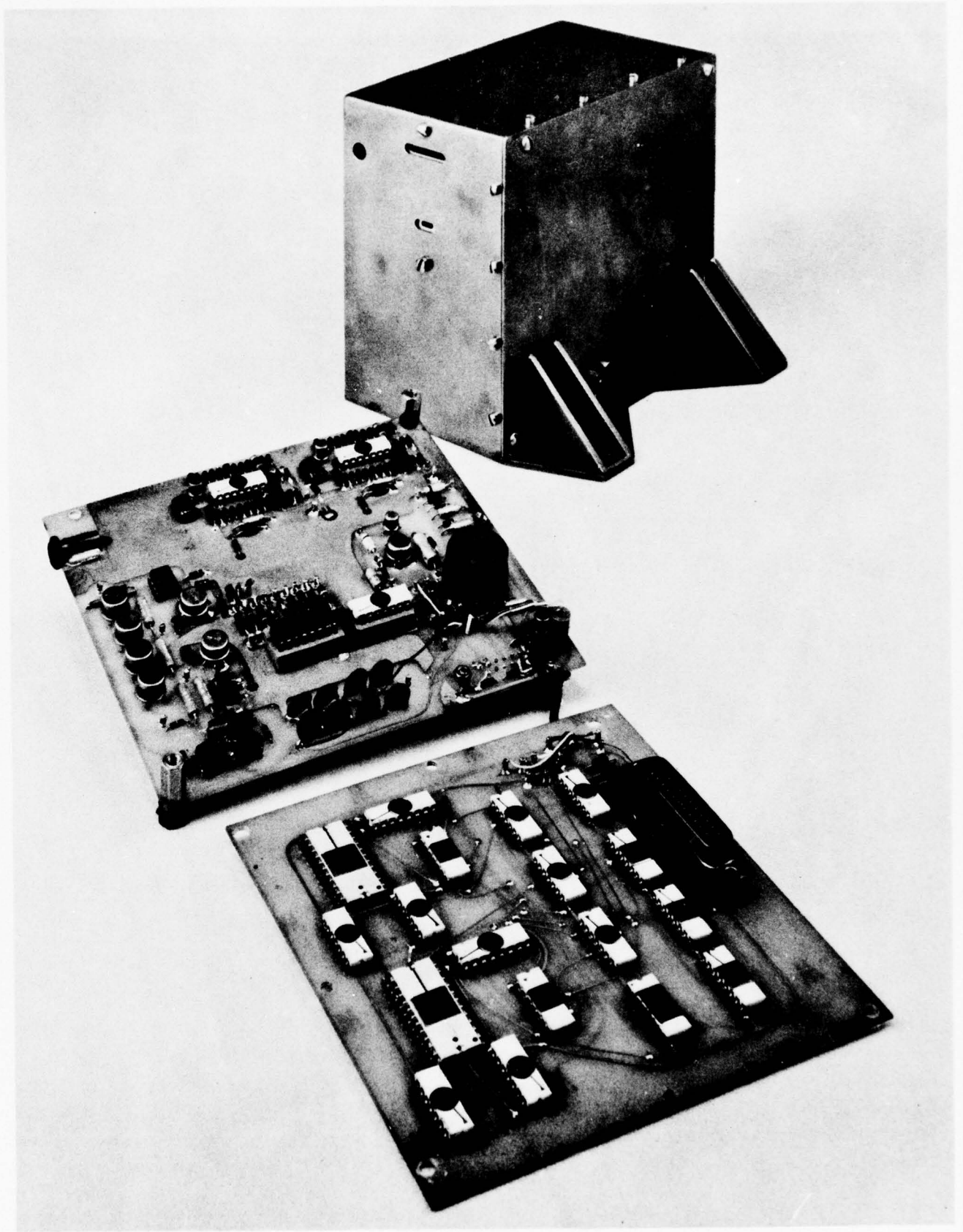


Fig. 1

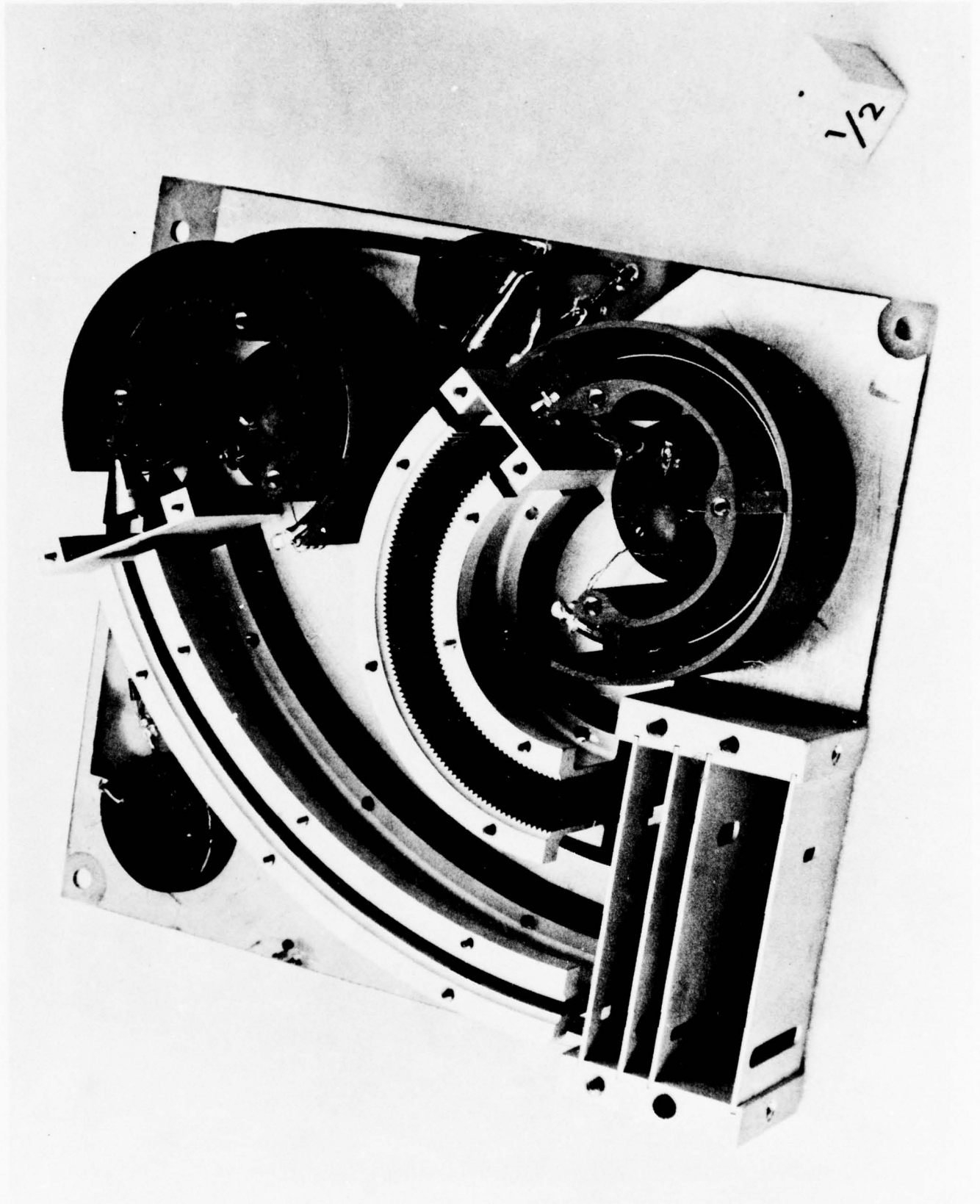


Fig. 2

SSJ/3 ESA ASSEMBLY

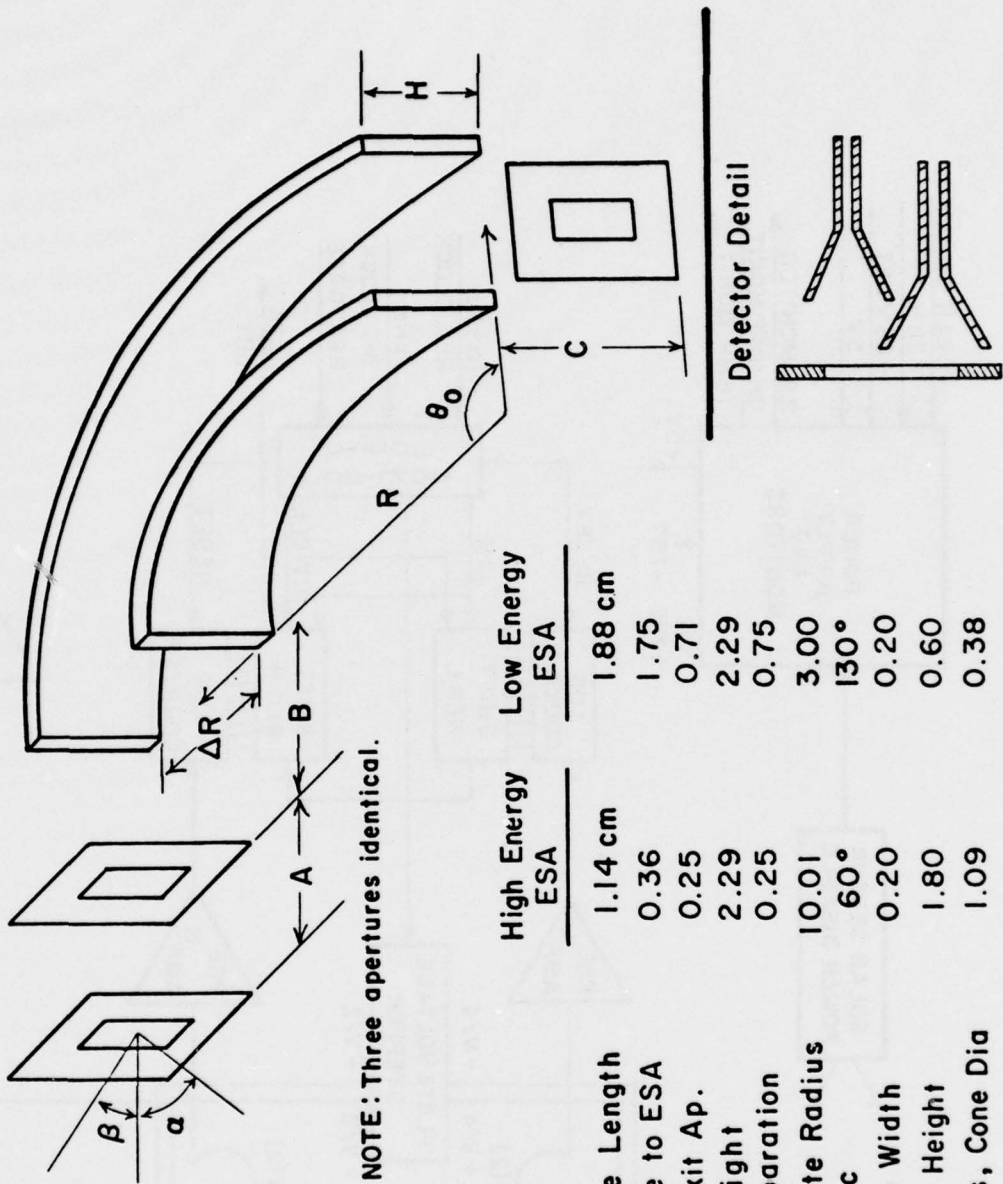


Fig. 3

SSJ/3 BLOCK DIAGRAM

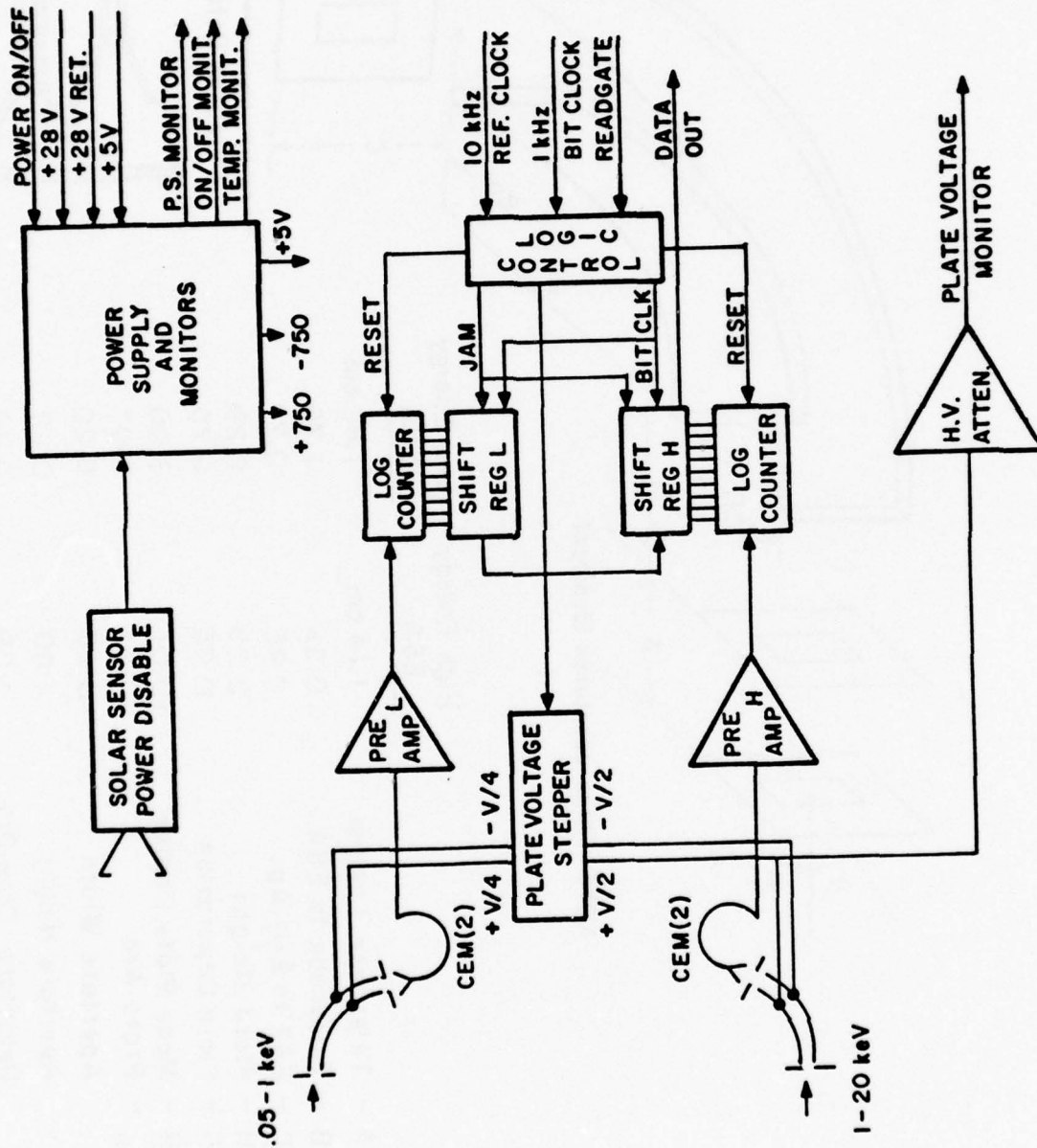


Fig. 4

ENERGY RESPONSE NORMALLY INCIDENT AND MONOENERGETIC BEAM

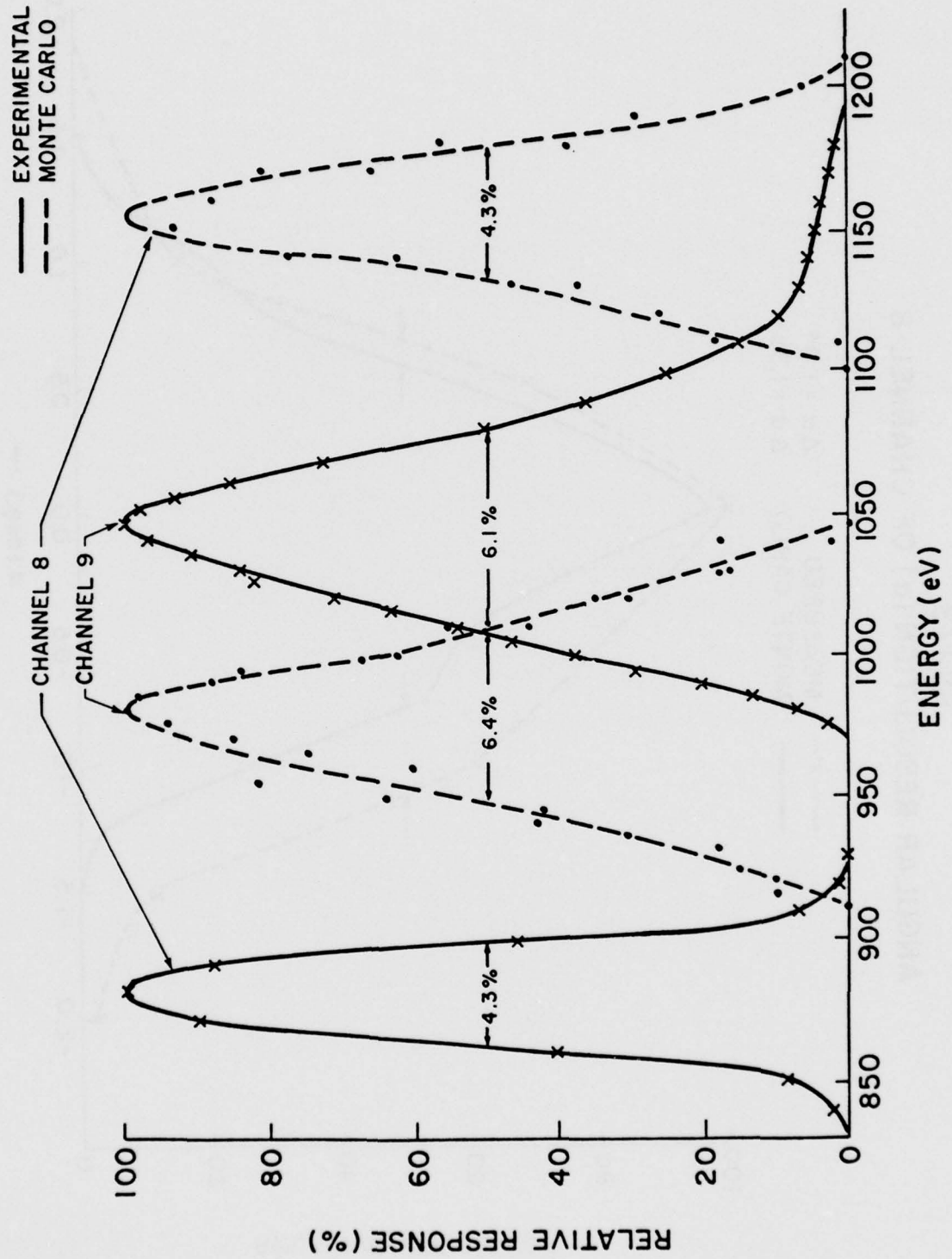


Fig. 5

SSJ/3
 ANGULAR RESOLUTION (α) OF CHANNEL 8

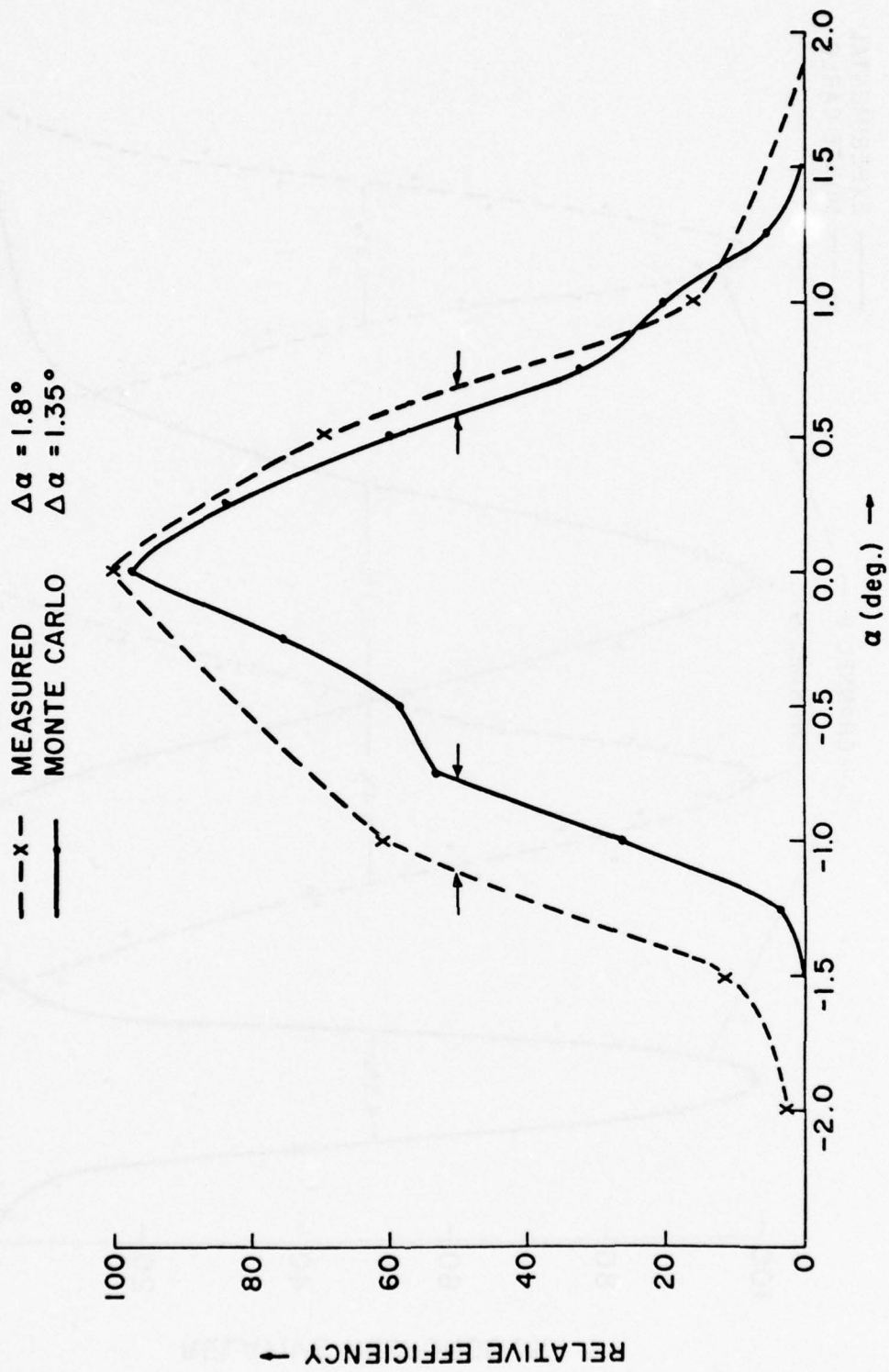


Fig. 6

ANGULAR RESOLUTION (α) OF SSJ/3
ENERGY CHANNEL 9

MONTE CARLO $\Delta\alpha = 4.5^\circ$ MONTE CARLO
DATA $\Delta\alpha = 3.7^\circ \pm 0.7$ MEASURED

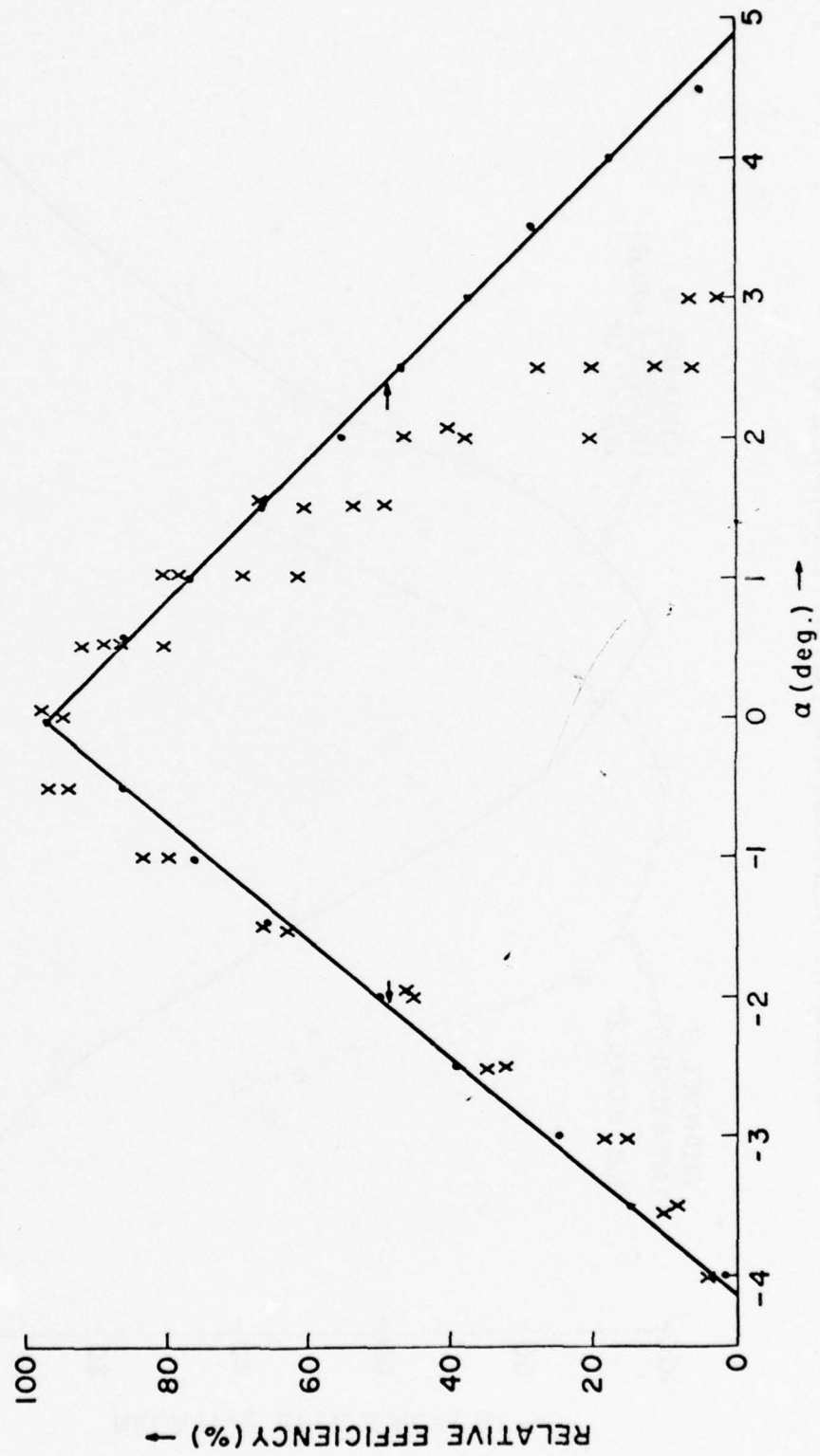


Fig. 7

SSJ / 3
 ANGULAR RESOLUTION (β) OF CHANNEL 8

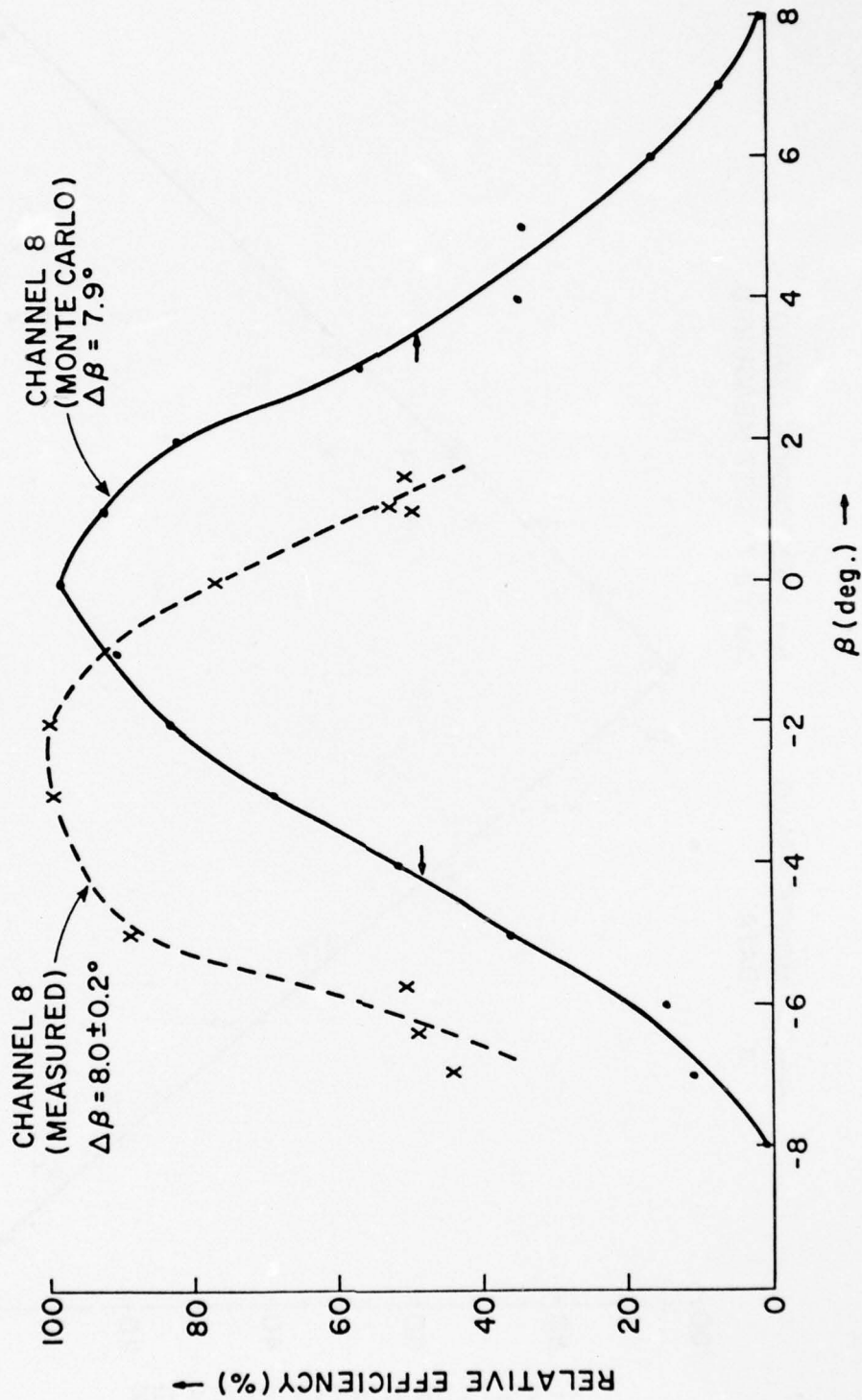


Fig. 8

ANGULAR RESOLUTION (β) OF SSJ/3
ENERGY CHANNEL 9

---x--- MEASURED $\Delta\beta = 4.75 \pm 0.08^\circ$
 —●— MONTE CARLO $\Delta\beta = 3.0^\circ$

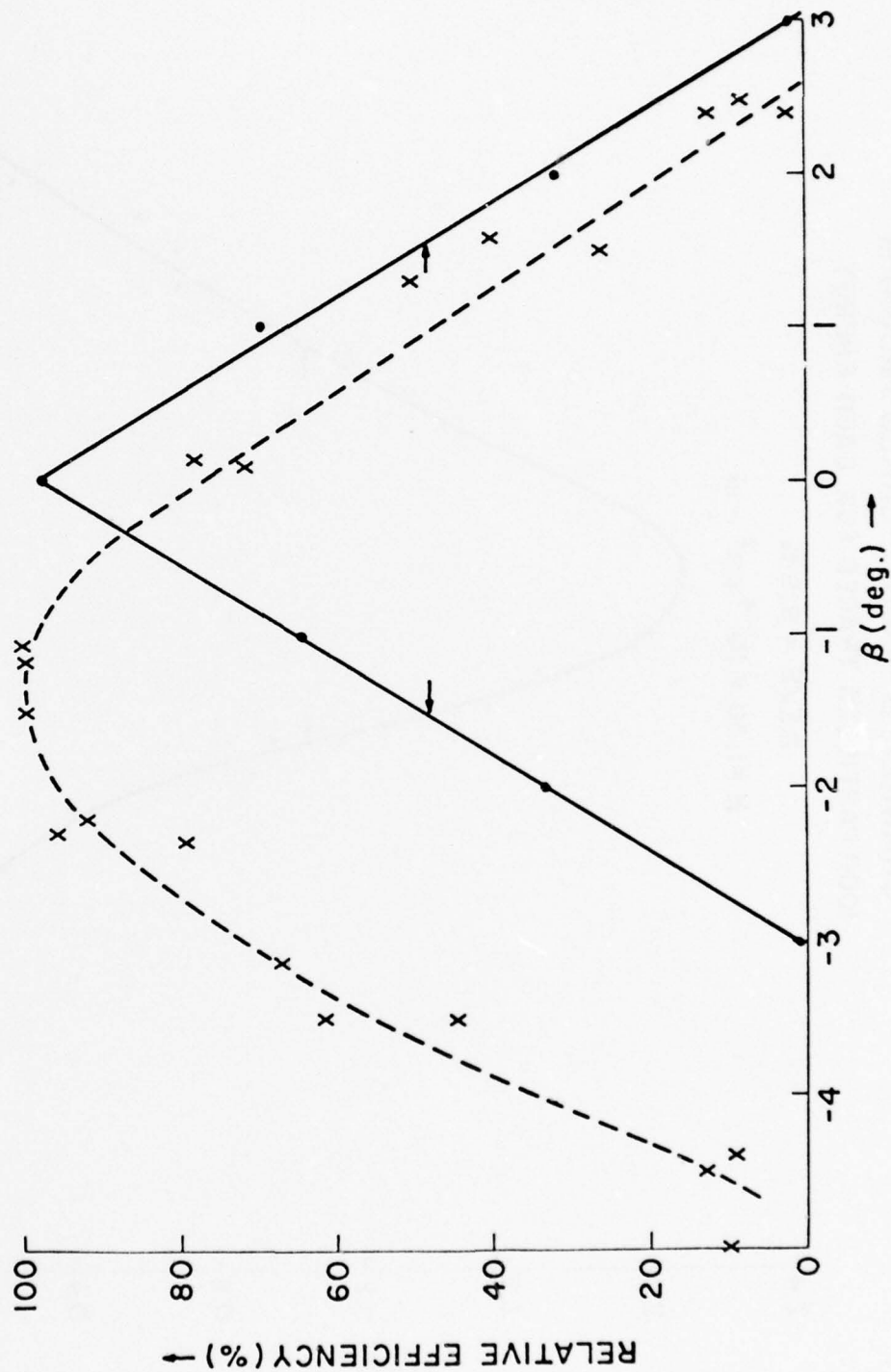


Fig. 9

ENERGY RESPONSE - ISOTROPIC INCIDENT FLUX
CHANNEL 8 - MONTE CARLO PROGRAM
1000 PARTICLES TRACED FOR EACH ENERGY

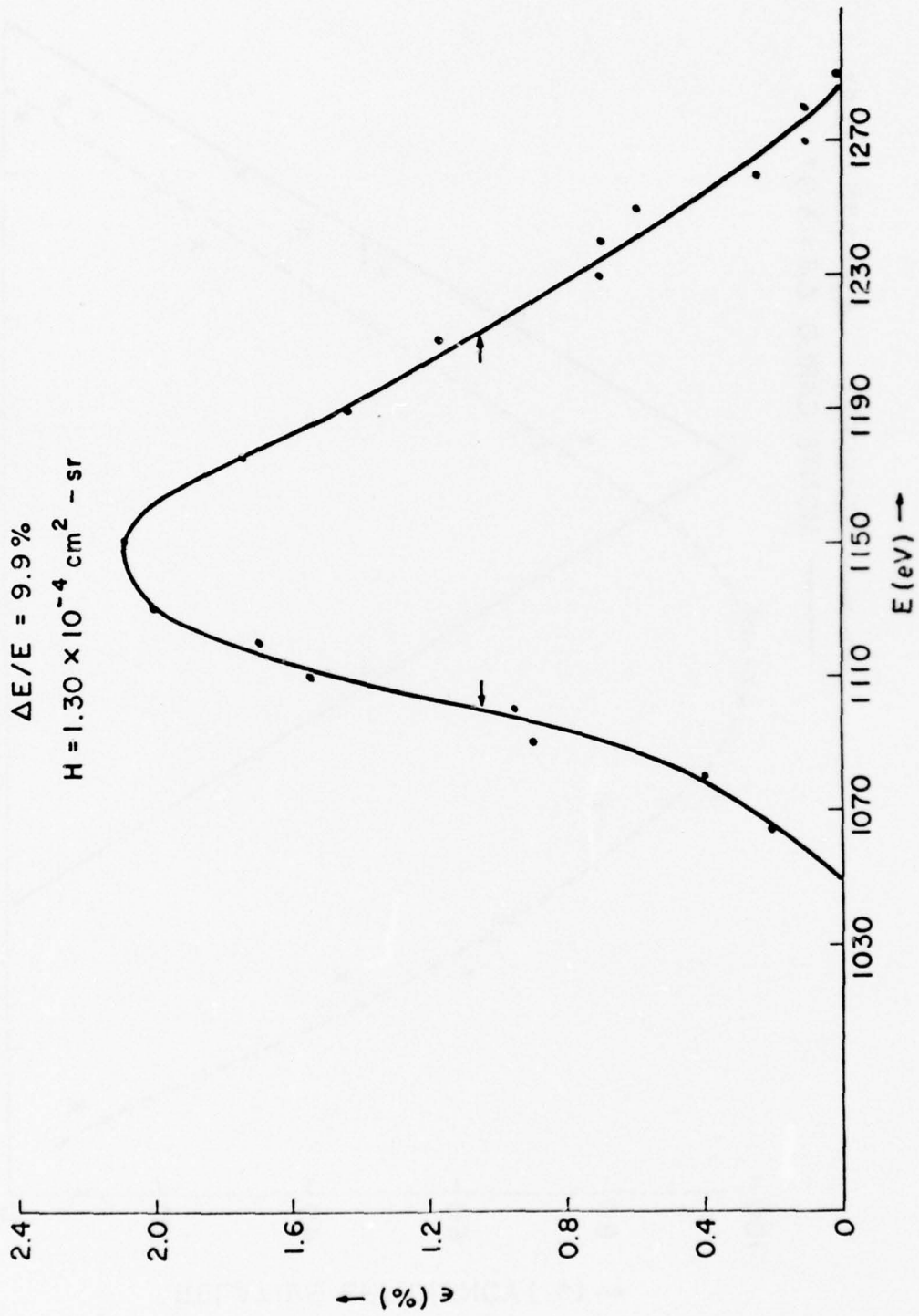


Fig. 10

ENERGY RESPONSE - ISOTROPIC INCIDENT FLUX
CHANNEL 9 - MONTE CARLO PROGRAM

1000 PARTICLES TRACED FOR EACH ENERGY

$$\Delta E/E = 9.2\%$$

$$H = 4.3 \times 10^{-5} \text{ cm}^2 \text{ - sr}$$

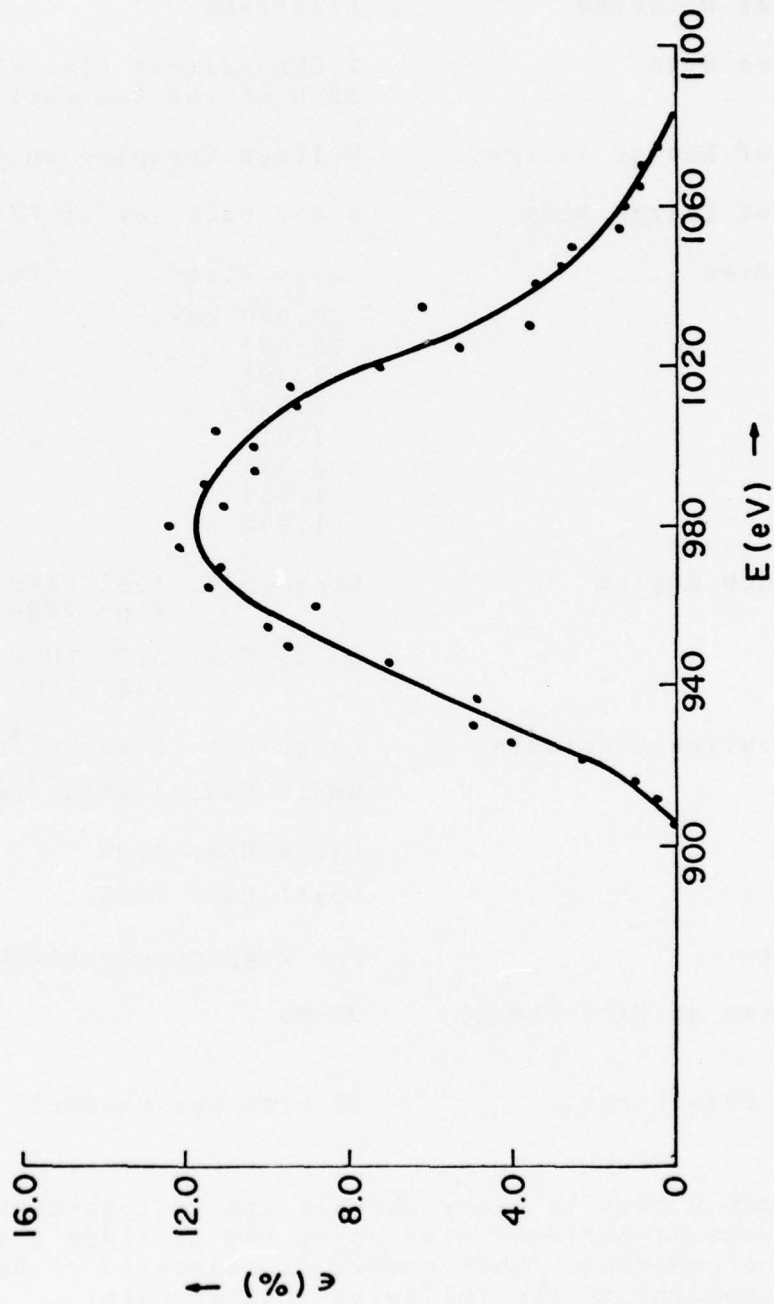


Fig. 11

APPENDIX A
ELECTROSTATIC ANALYZER (ESA)
SSJ/3 OR GFE3

Summary of Characteristics

Particles Detected	Electrons	
Detectors Used	2 Channeltron Electron Multipliers for each of the two sets of ESA plates	
Method of Energy Analysis	Voltage Stepping on ESA plates	
Number of Energy Bins	8 for each set of ESA plates; total of 16	
Energy Bins	Large Plates	Small Plates
	20.000 keV	1.000 keV
	13.037	.652
	8.498	.425
	5.539	.277
	3.611	.181
	2.354	.118
	1.534	.077
	1.000	.050
Acceptance Angles	Large ESA: 1.6° FWHM across the apertures 8.0° FWHM along the apertures	
	Small ESA: 3.7° FWHM across the apertures 4.8° FWHM along the apertures	
Normalization Constants	Large ESA: $1.30 \times 10^{-4} \text{ cm}^2\text{-ster.}$	
	Small ESA: $4.3 \times 10^{-3} \text{ cm}^2\text{-ster.}$	
$\frac{\Delta E}{E}$	Large ESA: 4.0%	
	Small ESA: 7.2%	
Data Rate	One complete Spectrum per second	
Dwell Time at Each Energy Level	98 ms.	
Digital Data Format	(9 bits per channel) x (16 channels) = 144 bits	

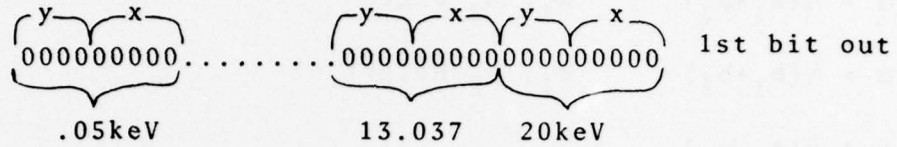
Note: Each 9 bits in every channel are in logarithmic form, the five least significant bits being the mantissa and the remaining four the exponent. This number is converted to decimal form according to the following relationship:

$$N = 2^y(x+32) - 33$$

where; 0000000000 ^{←LSB}
 y x

Data Readout

The first bit to be read out is the least significant bit (LSB) of the highest channel followed by the next to the highest one etc., i.e.:



[.....144 bits.....]
 read out in one group
 at the end of each second

Analog Monitors

Plate voltages: 5.0 volts to .25v
 Power supply : 2.5v
 Temperature : 2.5v at room temperature

Size

5.50in X 3.39in X 5.10in

Weight

3.046 lbs

Power Dissipation

.125 watts

APPENDIX B

The G-factor for a rectangular shaped collimator can be calculated exactly (Rothwell and Moomey, 1972). With the front and rear apertures having the dimensions (a_1, b_1) and (a_2, b_2) respectively, one can define

$$\begin{aligned}\alpha &= \frac{1}{2}(a_1 + a_2) && a_1, a_2 \text{ width} \\ \beta &= \frac{1}{2}(b_1 + b_2) && b_1, b_2 \text{ height} \\ \gamma &= \frac{1}{2}(a_1 - a_2) \\ \delta &= \frac{1}{2}(b_1 - b_2)\end{aligned}$$

If the collimator has a length L then

$$\begin{aligned}G &= L^2 \ln \left[\frac{L^2 + \alpha^2 + \delta^2}{L^2 + \alpha^2 + \beta^2} \cdot \frac{L^2 + \gamma^2 + \beta^2}{L^2 + \gamma^2 + \delta^2} \right] \\ &\quad + F(\alpha, \beta) + F(\gamma, \delta) - F(\alpha, \delta) - F(\gamma, \beta)\end{aligned}$$

where $F(\alpha, \beta) = F(\alpha, \beta) + F(\beta, \alpha)$

$$F(\alpha, \beta) = 2\beta(L^2 + \alpha^2)^{\frac{1}{2}} \tan^{-1} \left[\frac{\beta}{(L^2 + \alpha^2)^{\frac{1}{2}}} \right]$$

This expression is consistent with that given by Willis and Thomas (1972) and by Sullivan (1971) (with a corrected typographical error).

APPENDIX C

Listing of computer code that was used for the Monte-Carlo computations.

```

PROGRAM ESAPLTS(INFUT,OUTPUT)                                10
  DIMENSION DAT(24),EFF(200),EE(200),EG(200),AMAT(10,10),S   11
+UM1(10)                                                    11
  DIMENSION THH(100),AX(100),THM(100)                       12
  COMMON/F1/EFF,EG,DELE,N5,GINT                              13
  R2(X)=A*X+B                                                14
  F(X,Y,AL)=2.0*Y*SQRT(AL**2+X**2)*ATAN(Y/SQRT(AL**2+X**2)) 15
  N5=60                                                       16
  N7=N5/6                                                     17
  N9=5                                                         18
  N11=30                                                       19
  N12=N11/2                                                   20
  AMP=1.66E-27                                                21
  QOVMP=9.638E 07                                             22
  AME=9.1E-31                                                 23
  QOME=1.7582E 11                                            24
  AA=180./3.141596                                           25
  CNNTA=0.0                                                   26
  ELEC=8*PI*ELECTRON                                         27
1  CONTINUE                                                  28
  CALL RANSET(TIME(DUM))                                       29
  CNNTA=0.0                                                   30
C IF II=1 DC BACKGROUND CALCULATION BASE ON "LINE OF SIGHT" 31
C  IJ.NE. 0, AUTOMATICALLY ASSUMES PARAMETERS FOR L. FRANKS E 32
+SA                                                           32
C IJ=2, SIMULATES ELECTRON GUN SCAN OF FRANKS ESA AS SHOWN IN F 33
+IG. 2 OF                                                    33
C HIS PAPER                                                 34
C II=1, DOES LINE OF SIGHT BACKGROUND CALCULATION           35
C K1=0, NO ELASTIC SCATTERING OFF OF ESA PLATES              36
C K1=1, MORE THAN 1 SCATTERING OFF OF ESA PLATES PER ELECTRON A 37
+S DEFINED                                                  37
C BY K2 (INNER PLATE)                                       38
C K1=2, 1/K2X100 PER CENT SCATTERING OFF OF ESA PLATES (INNER P 39
+LATES)                                                      39
C K1=3, SCATTERING OFF OF OUTER ESA PLATE AS DEFINED BY K9  40
C K1=4, SCATTERING OFF OF OUTER ESA PLATE AS DEFINED BY 1/K9X100 41
C K1=5, SCATTERING OFF OF BOTH PLATES, K2 TIMES INNER PLATE, K9 T 42
+IMES OFF                                                    42
C ATE                                                        43
C K1=6, SCATTERING OFF OF BOTH PLATES 1/K2 INNER, 1/K9 TIMES OUTER 44
+PLATE                                                       44
C IF IK=0 INCIDENT FLUX IS ISOTROPIC                        45
C IK=1 INCIDENT FLUX AT INCIDENT ANGLE ANGE                 46
C IF IK=2 SCAN IN R-PLANE IN STEPS OF ANGE DEGREES         47
C IF IK=3 SCAN IN Z-PLANE IN STEPS OF ANGE DEGREES         48
C NOTE-- IF IK GE 2 INPUT DATA PACK CHANGES              49
  READ 4,II,IJ,K1,K2,K9,ANGA,ANG2,ANGD,IK,ANGE              50
4  FORMAT(5I5,3F7.2,I5,F7.2)                                 51
  PRINT 1900,IK,ANGE                                         52
1900 FORMAT(1X,I5,F7.2)                                       53

```


	IF(K1.EQ.0) K7=1	54
	IF(K1.EQ.1) K7=1	55
	IF(K1.EQ.2) K7=1	56
	IF(K1.EQ.3) K7=2	57
	IF(K1.EQ.4) K7=3	58
	IF(K1.EQ.5) K7=2	59
	IF(K1.EQ.6) K7=3	60
	IF(K1.EQ.0) K8=1	61
	IF(K1.EQ.1) K8=2	62
	IF(K1.EQ.2) K8=3	63
	IF(K1.EQ.3) K8=1	64
	IF(K1.EQ.4) K8=1	65
	IF(K1.EQ.5) K8=2	66
	IF(K1.EQ.6) K8=3	67
	IF(K1.EQ.7) K7=2	68
	IF(K1.EQ.7) K8=3	69
	IF(K1.EQ.8) K7=3	70
	IF(K1.EQ.8) K8=2	71
	READ 3, (DAT(I), I=1,24)	72
3	FORMAT((12A6))	73
	READ2, PART, POST	74
2	FORMAT(A8, F8.0)	75
	PRINT 5, (DAT(I), I=1,24)	76
5	FORMAT(1F1, 12A6/12A6)	77
	IF(II.EQ.1) FRINT 10	78
10	FORMAT(1X,*BACKGROUND CALCULATION*)	79
	IF(IK.EQ.1) PRINT 12, ANGE	80
12	FORMAT(1X,* CONST. ANGLE SORT, ANGLE=*, F7.2, * DEG.*)	81
	IF(PART.EQ.ELEC) AMP=AME	82
	IF(PART.EQ.ELEC) GOVMF =-OOME	83
	PRINT 6, PART	84
6	FORMAT(1X,*TRACING*, 3X, A8/)	85
	IF(PART.EQ.ELEC.ANC.IJ.NE.0) POST=160.	86
	IF(IJ.NE.0) PRINT 16	87
16	FORMAT(1X,* FRANKS ESA *)	88
	IF(IJ.EQ.2) FRINT 18	89
18	FORMAT(1X,*ELECTRON GUN FLUX=2.0E 06 ELEC/CMSG/SEC*)	90
	IF(K1.NE.0) FRINT 17, K1, K2, K9	91
17	FORMAT(1X,*ELASTIC SCATTERING OFF OF ESA PLATES ,*,	92
	++K1=*, I5,	92
	A * K2=*, I5/1X,*IF K1=1 K2 SCATTERINGS PER PART., IFK1=2	93
	+ EVERY OT	93
	BHER K2 PART. MAY SCATTER*, *K9=*, I5)	94
	IF(K1.NE.0) PRINT 21, ANG2	95
	IF(K1.NE.0) PRINT 19, ANGA	96
	IF(K1.NE.0) PRINT 23, ANGD	97
19	FORMAT(1X,* MAX SCATTERING ANGLE OFF OF OUTER PLATE=*, F7.	98
	+2,* DEG*)	98
21	FORMAT(1X,* MAX SCATTERING ANGLE OFF OF INNER PLATE=*, F7.	99
	+2,* DEG*)	99
23	FORMAT(1X,*MAX. ANGLE FOR INELASTIC SCATTERING OFF OF OU	100
	+TEF PLATE	100

	A=*,F7.2)	101
C	SET-UP APERTURE AND CALCULATE ITS G-FACTOR	102
	READ 8,A1,B1,A2,B2,AL1,AL2,AL3,VOLT1,R5	103
6	FORMAT(7F7.3,2F7.3)	104
	PRINT 11,A1,B1,A2,B2,AL1,AL2,AL3,VOLT1,R5,POST	105
11	FORMAT(1X,*APERTURE DIMENSIONS*/1X,*FRONT WIDTH=*,F7.3,* C	106
	+M*,3X,*FR	106
	10NTHT=*,F7.3,* CM*,3X,*BACK WIDTH=*,F7.3,* CM*,3X,*BACK	107
	+HT=*,F7.3	107
	2,*CM*/1X,*LENGTH OF APER.=*,F7.3,* CM*,3X,*DIST BTWN APE	108
	+R AND FLA	108
	3TFS=*,F7.3,* CM*/1X,*DIST BTWN PLATES AND CHANN.=*,F7.3,*	109
	+ CM*,3X,*	109
	4BIAS VOLTAGE IN FRONT OF DETECT.=*,F7.1,* VOLTS*/1X,*CHAN	110
	+NELTRON R	110
	1ADIUS=*,F7.2,* CM*,* POST ACCELERATION=*,F8.0,*VOLTS*/1)	111
	ALPHA=(A1+A2)/2.0	112
	BETA=(B1+B2)/2.0	113
	GAM=(A1-A2)/2.0	114
	DELTA=(B1-B2)/2.0	115
	G1=AL1**2*ALOG((AL1**2+ALPHA**2+DELTA**2)*(AL1**2+GAM**2+	116
	+BETA**2)/	116
	1(AL1**2+ALPHA**2+BETA**2)/(AL1**2+GAM**2+DELTA**2))	117
	G2=F(ALPHA,BETA,AL1)+F(BETA,ALPHA,AL1)+F(GAM,DELTA,AL1)+F	118
	+(DELTA,GAM	118
	1M,AL1)-F(ALPHA,DELTA,AL1)-F(DELTA,ALPHA,AL1)-F(GAM,BETA,A	119
	+L1)-F(PET	119
	2A,GAM,AL1)	120
	G=G1+G2	121
	PRINT 13,G	122
13	FORMAT(1X,*G-FACTOR FOR APERTURE=*,E10.4,* CMSQ-SR*/1)	123
	PRINT 15	124
15	FORMAT(1X,*ESA PLATE DIMENSIONS*)	125
C	R2A=RADIUS AT APERTURE	126
C	R2B=RADIUS AT EXIT	127
	READ 7,R1,R2A,R2B,THE,VOLT,H,TOT,R9	128
7	FORMAT(4F7.3,E10.2,F7.3,E10.4,F7.2)	129
	PRINT 9,R1,R2A,R2B,THE,VOLT,H,TOT,R9	130
9	FORMAT(1X,*ZERO POTENTIAL RADIUS=*,F7.3,*CM*,3X,*RADIUS A	131
	+T POTENTI	131
	1AL V AT APERTURE=*,F7.3,* CM*,3X,*RADIUS AT POTENTIAL V A	132
	+T EXIT=*,	132
	2F7.3,* CM*/3X,*MAX. ANGLE OF PLATES=*,F7.2,* DEGS*,3X,*VO	133
	+LTAGE ON	133
	3 PLATES=*,1PE10.2,* VOLTS*/3X,*PLATE HEIGHT=*,0PF7.2,*	134
	+CM*,* N	134
	4UMBER OF PARTICLES TRACED FOR EACH ENERGY=*,1PE10.2/1X,*D	135
	+ISTANCE 0	135
	5F CHANNELTRON FROM CENTER OF ESA AXIS=*,1PE10.2,* CM*/1)	136
	IF(PART.EQ.ELEC) VOLT =-VOLT	137
	THE=THE/AA	138

BEST AVAILABLE COPY

H=H*1.0E-02	139
ANGR=ANGA/AA	140
ANGC=ANG2/AA	141
ANGD=ANG0/AA	142
ANGE=ANGE/AA	143
R1=P1*1.0E-02	144
R2A=R2A*1.0E-02	145
R2B=R2B*1.0E-02	146
R5=R5*1.0E-02	147
R9=R9*1.0E-02	148
B=R2A	149
A= (R2B-R2A)/THE	150
WIG1=AES(R2A-R1)	151
RR=(R1+R2B)/2.0	152
A1=A1*1.0E-02	153
B1=B1*1.0E-02	154
A2=A2*1.0E-02	155
B2=B2*1.0E-02	156
AL1=AL1*1.0E-02	157
AL2=AL2*1.0E-02	158
AL3=AL3*1.0E-02	159
R6=RR-A1/2.0	160
R7=RR-A2/2.0	161
R8=RR+A2/2.0	162
IF(IJ.NE.0) R6=1.24E-01	163
IF(IJ.NE.0) R7=R6	164
IF(IJ.NE.0) R8=R6+A2	165
IF(IJ.EQ.2) THY=-5.0/AA	166
DELY=1.0/AA	167
THW=THY-DELY	168
THX=THE/2.0	169
R3=P2(THX)	170
GO TO 14	171
24 IF(IK.GE.2) READ 26,VOLT	172
IF(IK.GE.2) PRINT 29,VOLT	173
26 FORMAT(1PE10.2)	174
29 FORMAT(1X,* VOLTAGE ON PLATES=*,1PE10.2,* VOLTS*)	175
IF(PART.EQ.ELEC) VOLT =-VOLT	176
14 CONTINUE	177
C USING MKS SYSTEM--ENERGY IN JOULES	178
EE(1)=VOLT/2.0/ALOG(R3/R1)*1.6E-19	179
EE(1)=ABS(EE(1))	180
CONST=QOVMP*VOLT	181
EA=EE(1)/1.6E-19	182
PRINT 31,EA	183
31 FORMAT(1X,*MEAN ENERGY=*,1PE10.2,*EV*)	184
IF(IK.LT.2) GO TO 34	185
THH(1)=-ANGE*N12	186
DO 33 I=1,N11	187
THH(I+1)=THH(I)+ANGE	188
THM(I)=THH(I)*AA	189

BEST AVAILABLE COPY

	AX(I)=0.0	197
33	C CONTINUE	191
	THH(N11+1)=THH(N11+1)*AA	192
	GO TO 36	193
34	CONTINUE	194
	DELE=0.005*EE(1)	195
	EE(1)=0.9*EE(1)	196
	DO 35 K=1,N5	197
	EE(K+1)=EE(K)+DELE	198
35	CONTINUE	199
36	CONTINUE	200
	DO 22 J=1,10	201
	DO 22 K=1,10	202
	AMAT(K,J)=0.0	203
22	CONTINUE	204
25	CONTINUE	205
	THW=THW+DELY	206
	THW=-4.0/AA	207
	DO 600 K=1,N5	208
	K13=1	209
37	CONTINUE	210
	K4=0	211
	N4=0	212
	N6=0	213
	K5=0	214
	CNT=0.0	215
	COUNT=0.0	216
	CNTA=0.0	217
C	DELTA=TIME INTERVAL FOR EACH STEP	218
	GO TO 40	219
38	IF(IK.GE.2) GO TO 202	220
40	CONTINUE	221
	K3=0	222
	N3=0	223
	K11=0	224
	K12=0	225
	EX=EE(K)	226
	IF(IK.GE.2) EE(K)=EA*1.6E-19	227
	V=SQRT(2.*EE(K)/AMP)	228
C	PULL OUT DEFOREST CARDS	229
	R=R6+A1*RANF(DUM)	230
	Z1=91*RANF(DUM)	231
C	CHOOSE T1 SUCH THAT FOR J(FLUX) = CONST. T1 IS PICKED SIN(T1*	232
	+COS(T1)	232
C	TIMES,, SIN FOR SOLID ANGLE COS FOR PROJECTED AREA	233
	T1=ACOS(1.0-2.0*RANF(DUM))/2.0	234
	T2=6.2831*RANF(DUM)	235
	IF(IK.EQ.1) T1=ANGE	236
	IF(IK.EQ.1) T2=0.0	237
	IF(IK.EQ.2) T1=THH(K13)	238
	IF(IK.EQ.2) T2=0.0	239

	IF(IK.EQ.3) T1=THH(K13)	240
	IF(IK.EQ.3) T2=1.5707	241
	IF(IJ.EQ.2) T1=ABS(THW)	242
	IF(IJ.EQ.2.AND.THW.GE.C.0) T2=180./AA	243
	IF(IJ.EQ.2.AND.THW.LT.0.0) T2=0.0	244
	Y1=0	245
	VR=V*SIN(T1)*COS(T2)	246
	VTT=V*COS(T1)	247
	VZ=V*SIN(T1)*SIN(T2)	248
	DT=AL1/VTT	249
	R=R+VR*DT	250
	Z1=Z1+VZ*DT	251
	IF(Z1.GT.B2.OR.Z1.LT.0.0) GO TO 38	252
	IF(R.GT.R8.OR.R.LT.R7) GO TO 38	253
	CNTA=CNLA+1.0	254
	DT=AL2/VTT	255
	R=R+VR*DT	256
	Z1=Z1+VZ*DT	257
	IF(R.GE.R2A.OR.R.LE.R1) GO TO 202	258
	ANGM=VTT*R	259
	TT1=0.0	260
	R3=R2(TT1)	261
	CONTT=CONST/ALOG(R3/R1)	262
	CONSS=CONST	263
	IF(II.EQ.1) CONSS=0.0	264
	DELTT=CONTT/(R1+R3)*2	265
	DELTT=3.E-01*V/DELTT	266
	DELT=3.1416*THE*(R1+R3)/2./V/2.0E 02	267
	IF(DELTT.LE.DELT) DELT=DELTT	268
	GO TO 20	269
27	CONTINUE	270
	IF(K12.GT.0.OR.K11.GT.0) R=R+VR*DELT	271
	GOTO 28	272
20	CONTINUE	273
	R3=R2(TT1)	274
	CONS2=(VTT**2-CONSS/ALOG(R3/R1))/R	275
	R=R+VR*DELT+CONS2*DELT**2/2.0	276
	VF=VR+CONS2*DELT	277
28	CONTINUE	278
	VTT=ANGM/R	279
	TT1=TT1+VTT*DELT/R	280
	Z1=Z1+DELT*VZ	281
	IF(Z1.LE.0.0.OR.Z1.GE.H) GOTO 202	282
	IF(TT1.GE.THE) GO TO 400	283
	IF(R.GT.R1.AND.R.LT.P3) GO TO 1700	284
	GO TO 1800	285
1700	CONTINUE	286
	K11=0	287
	K12=0	288
	GO TO 20	289
1800	CONTINUE	290

BEST AVAILABLE COPY

C	K1=1,2-----SCATTER OFF OF INNER SURFACE ONLY	291
C	K1=3,4----SCATTER OFF OF OUTER SURFACE ONLY	292
	IF(R.GE.R3) GO TO 1300	293
	IF(R.LE.R1) GO TO 1400	294
	GO TO 202	295
1300	CONTINUE	296
	IF(K11.GT.0) GO TO 27	297
	K11=K11+1	298
	GO TO (2(2,1100,1200),K7	299
1400	CONTINUE	300
	IF(K12.GT.0) GO TO 27	301
	K12=K12+1	302
	GO TO (202,900,1000),K8	303
900	CONTINUE	304
	N3=N3+1	305
	IF(N3.GT.K9) GO TO 202	306
	VD=ABS(VR)	307
	THP=ATAN(VD/VTT)	308
	IF(ABS(THP).GT.ANGC) GO TO 1500	309
	VF=-VR	310
	GO TO 27	311
1000	CONTINUE	312
	VD=ABS(VR)	313
	THP=ATAN(VD/VTT)	314
	N6=N6+1	315
	IF(ABS(THP).GT.ANGC) GO TO 1500	316
	VF=-VR	317
	GO TO 211	318
1100	CONTINUE	319
	VD=ABS(VR)	320
	K3=K3+1	321
	IF(K3.GT.K2) GO TO 202	322
	THP= ATAN(VR/VTT)	323
	IF(ABS(THP).GT.ANGC) GO TO 202	324
	IF(ABS(THP).GT.ANGE) GC TO 1600	325
	VF=-VR	326
	GO TO 27	327
1200	CONTINUE	328
	VD=ABS(VR)	329
	K4=K4+1	330
	THP= ATAN(VR/VTT)	331
	IF(ABS(THP).GT.ANGC) GO TO 202	332
	IF(ABS(THP).GT.ANGE) GO TO 1600	333
	VR=-VR	334
	GO TO 200	335
1500	CONTINUE	336
	EX=EX *(1.0-RANF(DUM))**(1.0/1.35)	337
	VA=SQRT(2.0*EX/AMP)	338
	VR=VA*SIN(THP)	339
	VTT=VA*CCS(THP)	340
	IF(K8.EQ.3) GO TO 201	341

	GO TO 27	342
1600	CONTINUE	343
	EX=EX *(1.0-RANF(DUM))**(1.0/1.35)	344
	VA=SQRT(2.0*EX/AMP)	345
	VR=-VA*SIN(THP)	346
	VTT=VA*COS(THP)	347
	IF(K7.EQ.3) GO TO 200	348
	GO TO 27	349
200	CONTINUE	350
	IAB=MCD(K4,K2)	351
	IF(IAB.EQ.0) K4=0	352
	K5=K4	353
	IF(IAB.EQ.0) GO TO 27	354
	GO TO 202	355
201	CONTINUE	356
	IAC=MCD(N6,K9)	357
	IF(IAC.EQ.0) N6=0	358
	N4=N6	359
	IF(IAC.EQ.0) GO TO 27	360
202	CONTINUE	361
	CNT=CNT+1	362
	IF(CNT.GE.TOT) GO TO 500	363
	GO TO 40	364
400	CONTINUE	365
C	SET UP MATRIX AT EXIT APERTURE OF FLATES	366
	DO 420 N=1,N9	367
	IF(Z1.GE.(N-1)*H/N9.AND.Z1.LT.N*H/N9) N1=N	368
420	CONTINUE	369
	DO 430 N=1,N9	370
	RRR1=R1+(N-1)*WID1/N9	371
	RRR2=R1+N*WID1/N9	372
	IF(R.GE.RRR1.AND.R.LT.RRR2) N2=N	373
430	CONTINUE	374
	AMAT(N1,N2)=AMAT(N1,N2)+1.0	375
C	DO WE HIT THE CHANNELTRON?	376
	RR=(R1+R2B)/2.0	377
C	FULL DEFOREST ESA CARDS	378
	DIS2=AL3	379
	DT=DIS2/VTT	380
	XX=0.0	381
	VXX=VTT	382
	VT=VOLT1	383
	DTT=0.1*DT	384
	TT=0.0	385
	ACC=QC*VMP*VT/DIS2	386
460	CONTINUE	387
	TT=TT+DTT	388
	XX=XX+VXX*DTT-ACC*DTT**2/2.0	389
	VXX=VXX-ACC*DTT	390
C	DOES LOW-ENERGY ELECTRON STOP	391
	IF(VXX.LE.0.0) GO TO 202	392

	IF (XX.LT.0IS2) GO TO 460	393
	R=F+VP*TT	394
	Z1=Z1+VZ*TT	395
	IF (IJ.NE.0) R5=1.77E-03	396
	IF (IJ.NE.0) R9=-R5	397
	R4=ABS(RR-R9-R)	398
C	PULL OUT DEFOREST CARDS	399
	IF (R.LT.(RR-A2/2.0).OR.R.GT.(RR+A2/2.0)) GO TO 202	400
	IF (Z1.GT.B2.OR.Z1.LT.C.0) GO TO 202	401
	P4A=SQRT(R4**2+(Z1-B2/2.0-R5)**2)	402
	R4B=SQRT(R4**2+(Z1-B2/2.0+R5)**2)	403
	IF (R4A.GT.R5.AND.R4B.GT.R5) GO TO 202	404
	IF (IK.GE.2) AX(K13)=AX(K13)+1.0	405
	COUNT=COUNT+1	406
	GO TO 202	407
500	CONTINUE	408
	EFF(K)=COUNT/CNT	409
	IF (IK.GE.2) AX(K13)=AX(K13)/CNT	410
	EG(K)=EE(K)/1.6E-19	411
	CNNTA=CNNTA+CNNTA	412
	PFINT 5(7,EG(K),CNNTA,CNNTA	413
507	FORMAT(1X,* AT ENERGY = *,1PE10.2,* EV NUMBER OF PA	414
	+ARTICLES	414
	1 THROUGH APERTURE = *,0PF10.2,* RUNNING TOTAL = *,0PF10.2)	415
	IF (II.EQ.1) GO TO 630	416
	E99=EG(K)/1.0E 03	417
	EFI=1.0	418
	TEMP=EG(K)	419
	EG(K)=EG(K)-VT+POST	420
	IF (PART.EQ.ELEC.AND.EG(K).GE.1.0E 03.AND.EG(K).LE.5.0E 0	421
	+6)	421
	1 EFI=1.0-(2.0/(3.0+6.5/(E99 -0.5)+30./(E99 -0.5)**3))	422
	IF (PART.EQ.ELEC.AND.EG(K).GE.1.0.0.AND.EG(K).LE.70.) EFI=0	423
	+ .10*EG(K)	423
	1**0.515	424
	IF (PART.EQ.ELEC.AND.EG(K).GE.200.AND.IJ.NE.0) EFI=8.199/EG	425
	+(K)**0.41	425
	A7	426
	IF (PART.EQ.ELEC.AND.EG(K).LT.200.AND.IJ.NE.0) EFI=5.9E-04*	427
	+EG(K)**1.	427
	A38	428
	EG(K)=TEMP	429
	IF (IK.GE.2) AX(K13)=AX(K13)*EFI	430
	IF (IK.GE.2) GO TO 440	431
	EFF(K)=EFF(K)*EFI	432
	IF (IJ.EQ.2) EFF(K)=EFF(K)*2.0E 06	433
	IF (MCD(K,N7).NE.C) GO TO 440	434
	E1=EE(K-N7+1)/1.6E-19	435
	E2=EE(K)/1.6E-19	436
	AN7=N7	437
	DO 435 N=1,N9	438

	SUM1(N)=0.0	439
	DO 435 I=1,N9	440
	SUM1(N)=SUM1(N)+AMAT(I,N)	441
435	CONTINUE	442
	AN8=N7*TOT	443
	PRINT 433,E1,E2,((AMAT(N1,N2),N2=1,N9),N1=1,N9),(SUM1(N),	444
	+N=1,N9),	444
	1AN8	445
433	FORMAT(1X,*EFFICIENCY MATRIX FOR EXIT APERTURE OF ESA FLA	446
	+TES FRCM	446
	1ENERGY=*,1PE10.2,*EV*,*TO*,1PE10.2,*EV*/0P5F10.2/5F10.2/5	447
	+F10.2/5F1	447
	Z0.2/5F10.2/1X,*TOTALS*/5F10.2,*PARTICLES TRACED=*,1PE10.2	448
	+//)	448
	DO 438 I=1,10	449
	DO 438 N=1,10	450
	AMAT(I,N)=0.0	451
438	CONTINUE	452
440	CONTINUE	453
	IF(IK.GE.2) K13=K13+1	454
	IF(IK.GE.2.AND.K13.LT.N11) GO TO 37	455
	IF(IK.GE.2) GO TO 610	456
	GO TO 600	457
600	CONTINUE	458
	CALL SIMP	459
610	CONTINUE	460
	IF(IK.EG.3) PRINT 613	461
613	FORMAT(1X,*ANGULAR SCAN IN Z-PLANE*)	462
	IF(IK.EQ.2) PRINT 609	463
609	FORMAT(1X,*ANGULAR SCAN IN R-PLANE*)	464
	IF(IK.GE.2) PRINT 611, (THM(K),AX(K),K=1,N11)	465
611	FORMAT((1P12E10.2))	466
	IF(IK.GE.2) GO TO 24	467
630	CONTINUE	468
	THR=THW*AA	469
	IF(IJ.EQ.2) PRINT 740,THR	470
740	FORMAT(1X,*ELECTRONS FROM GUN INCIDENT ON APERTURE AT AN	471
	+ANGLE OF	471
740 A	*,F7.2,* DEG*)	472
	PRINT 51	473
51	FORMAT(1X,*EFFICIENCY OF CHANNELTRON TO SEE PARTICLES*)	474
	PRINT 55,(EG(K),EFF(K),K=1,N5)	475
55	FORMAT(1X,*ENERGY-EFFICIENCY*/(1P10E12.2))	476
	G1=G*GINT	477
	PRINT 63,GINT,G1	478
63	FORMAT(1X,*INTEGRAL OF CHANN. EFFIC.=*,1PE10.4,* EV*,3X,*	479
	+NORMALIZA	479
	TION FACTOR FOR ENTIRE ESA=*,1PE10.4,* CMSQ-SR-EV*)	480
	HH=G1/EA	481
	PRINT 67,HH	482
67	FORMAT(1X,*DEFOREST H-FACTOR=*,1PE10.4,* CMSQ-SR*)	483
	GO TO 1	484
	END	485

BEST AVAILABLE COPY

	SUBROUTINE SIMP	466
	DIMENSION EFF(200),EG(200)	487
	COMMON/F1/EFF,EG,DELE,N5,GINT	488
C	SIMPSON RULE	489
	DEL=DELE/1.6E-19	490
	N6=N5-3	491
	N7=N5-2	492
	SUM1=0.0	493
	DO 10 J=3,N6,2	494
	SUM1=SUM1+EFF(J)	495
10	CONTINUE	496
	SUM2=0.0	497
	DO 20 J=2,N7,2	498
	SUM2=SUM2+EFF(J)	499
20	CONTINUE	500
	GINT=(EFF(1)+EFF(N5-1)+4.0*SUM2+2.0*SUM1)*DEL/3.0	501
	RETURN	502
	END	503

BEST AVAILABLE COPY

REFERENCES

- Pantazis, John; Huber, Alan; and Hagan M.P., Design of Electrostatic Analyzer, AFGL-TR-77-0120, 1977.
- Archuleta, R.J. and DeForest, J.E., Efficiency of Channel Electron Multipliers for Electrons of 1-50 keV, Rev. of Sci. Instru., 42, 89-91, 1971.
- Willis, D.M. and Thomas, G.R., Geometric Factor of a Cosmic Ray Detector: Equivalence of Alternative Analytical Derivations, Eldo-Cecles/ESRO-Cess Scient. and Tech. Rev., 4, 101-102, 1972.
- Sullivan, J.D., Geometrical factor and directional response of single and multi-element particle telescopes, Instr. and Methods, 95, 5-11, 1971.
- Rothwell, Paul L., and Moomey, Wayne R., Calibration of a Magnetic Spectrometer Designed to Measure 0.1 -1.0 MeV Electrons in Space, AFCRL-72-0710, 1972.

